WPSA-PR(17) 19040

PT Lang et al.

A flexible pellet injection system for the tokamak JT-60SA: The final conceptual design

Preprint of Paper to be submitted for publication in
Fusion Science and Technology

This work has been carried out within the framework of the EUROfusion Consortium and has received funding from the Euratom research and training programme 2014-2018 under grant agreement No 633053. The views and opinions expressed herein do not necessarily reflect those of the European Commission.

A flexible pellet injection system for the tokamak JT-60SA: The final conceptual design

P. T. Lang 1), T. Nakano 2), L. Garzotti 3), B. Pégourié 4), B. Ploeckl 1), S. Sakurai 2)

1) Max-Planck-Institut für Plasmaphysik, Boltzmannstrasse 2, 85748 Garching, Germany
2) National Institutes for Quantum and Radiological Science and Technology, Mukouyama, Naka City, Ibaraki, 311-0193
3) CCFE, Culham Science Centre, Abingdon, Oxon, OX14 3DB, United Kingdom
4) CEA, IRFM, 13108 Saint-Paul-lez-Durance, France

E-mail contact of main author: peter.lang@ipp.mpg.de

Abstract.
The research plan of JT-60SA, a superconducting tokamak device currently under construction, requests a powerful pellet injection system for its particle fuelling and ELM pacing experiments. These investigations, foreseen to answer basic questions with respect to the operation of ITER and a future fusion power plant like DEMO, need pellets with flexible parameters delivered precisely and reliable for control purposes. Here, we present a conceptual design of this system, basing on classical pellet technology. Analysis showed pellets will show the best performance for fuelling and most likely also for ELM pacing when injected from the torus inboard side, despite the limited maximum pellet speed caused by this approach. This is due to constructional constraints rising from the fact the JT-60SA vacuum vessel is already under construction, enforcing inboard injection via a multi bend guiding tube system and limiting the maximum pellet speed to about 470 m/s. To match this boundary condition and fulfil the needs for precise control, a centrifuge accelerator has been chosen. Basing on the stop cylinder principle and equipped with a double accelerator arm, it can host up to 4 steady state ice extruders working simultaneously for pellet production. This way, all system requirements expressed in the research plan can be well covered, providing even some headroom for better flexibility during the planned investigations. Details of our design and the reasoning for the layout chosen will be provided in this paper.

I. Introduction:

A new superconducting tokamak is currently built under the Broader Approach Satellite Tokamak Programme run jointly by Europe and Japan, and under the Japanese national programme. Approaching already completion, this device JT-60SA is expected to start operation in 2020 [1]. It will then be at the forefront of the international fusion programme, supporting the ITER experimental programme as a satellite machine. In addition, it is expected to provide key information for the operational scenario of future DEMO fusion reactors, in particular for a steady-state, advanced performance design option. The start-up of operation of such a large experimental device is a challenging enterprise, requiring a broad set of preparation activities. They involve amongst others the elaboration of a Research Plan [2] and conception studies of diagnostics and sub-systems for e.g. heating, matter injection and pumping. Many of these activities are carried out in a coordinated way by a joint Japan-EU JT-60SA Research Unit, in close interaction with the JT-60SA project for the machine construction [1]. One activity of this kind was the conceptual design of the pellet injection system, requested to be elaborated in a dedicated study within 3 years. The outcome of this study, finalised in 2017, is presented in this paper.

Aim of the study was to find the best possible design for a pellet system covering the requirements formulated in the JT-60SA research plan. However, this design had also to take into account all the boundary conditions arising from the fact the tokamak facility is already under construction, thus imposing constraints for e.g. torus access and any installations inside or close to the vessel. The mission of the JT-60SA endeavour is to support the exploitation of ITER

and, by resolving key physics and engineering issues, the design of a EU-DEMO reactor. Consequently, the pellet system has to be been designed for all of the resulting research needs. Two major tasks have been dedicated to the pellet tool, managing the injection of cryogenic solid pellets formed from fuel into the plasma: providing the main particle source for the core plasma and ELM pacing as one of the key techniques considered for ELM mitigation.

Efficient core particle fuelling has to be applied for operation at high central densities in long pulse discharges in ITER and DEMO-relevant conditions. In ITER and EU-DEMO, operation at core densities close to or even beyond the Greenwald density n_{Gw} [3] is a must in order to maximize fusion power output. A loss of the demanded high confinement mode (H-mode) operation takes place when approaching n_{Gw} by simple gas fuelling. This behaviour is attributed to an edge density limit which however can easily be overcome by deep particle deposition enforced by pellets [4, 5]. Hence, the density profile (or density gradient) needs to be optimized and controlled keeping the core density high while simultaneously preserving edge conditions.

Edge localised modes (ELMs) are intense, short duration relaxation events occurring in the H-mode regime [6, 7, 8], releasing particles and energy which load plasma facing components. Scaled up to ITER, such loads would be unacceptable high [9]. ELMs can also play a beneficial role by removing impurities from the plasma [10]. Hence, control of the ELM frequency and if possible ELM mitigation will be a key issue in reactor compatible plasma scenarios. There are several proposed methods for externally triggering or pacing ELMs in order to influence their size and occurrence frequency [11]. One of them is pellet injection, found to work reliable in several devices [12, 13]. However, more recently conditions have been observed where pellets failed to achieve ELM control [14]. Thus, the pellet system design has to provide the capacity for investigations in order to clarify the triggering issue and, in case of a positive result, deliver pellets suitable for ELM frequency and size control.

Details of the expected design data of the pellets delivered in order to enable for specific physics investigations and engineering capabilities are already provided by the JT-60SA research plan. For the physics goals it is enlisted the high density operation in ITER and DEMO relevant plasmas, exploration if and how densities above the Greenwald density can be accessed, investigations of the power exhaust by developing radiation layers, particle balance studies and the ELM control. As well, pellets shall be applied for studies on the non-linearity of the ion and electron heat transport observed from cold/heat pulse propagations. Regarding the density control, pellet fuelling experiments will be carried out to demonstrate effective density control capability in different scenarios. Estimated from a steady-state particle balance analysis (assuming the particle confinement time of the particles fuelled is equal to that of the particles fuelled by the neutral beam) this will require a pellet particle flux of up to 6.4×10^{21} s^{-1}. This can be, as proposed in the research plan, realised by injecting of cylindrical pellet with a diameter Ø and length l of both 2.4 mm at a rate of 13 Hz. In the case that the particle confinement time of the pellet deposited particles is smaller, it is understood a higher pellet particle flux is required. To cover this potential needs, an ultimate pellet flux capability of 3.0×10^{22} s^{-1} is considered in the research plan, to be shared in case by up to three individual injectors.

The requested engineering deliverable is to serve as actuator for control on electron density and ELMs within an advanced real-time control scheme. In a staged approach, it has to be commissioned by quantifying the impact in open loop during the first research phase to prepare for closed-loop control experiments in the second research phase. A real-time frequency control for the plasma density feedback control is planned with one pellet injector delivering the reference pellet size of Ø = l = 2.4 mm at a maximum injection frequency of 20 Hz. For ELM pace making, a pellet frequency upgrade to 60 Hz is foreseen in the research plan. For studies of the isotope effects on plasma confinement and controllability of isotope ratio, pellets in combination with gas puffing have to actuate for controlling the amount of each species.

Using superconducting toroidal and poloidal field coils, the tokamak device will be capable of confining break-even-equivalent class high-temperature deuterium plasmas lasting for a duration of typically 100 s, longer than the time scales characterizing key plasma processes, such as current diffusion and particle recycling. It has been designed to realize a wide range of diverted plasma equilibrium configurations, covering a wide range of different plasma scenarios. Six reference scenarios representing the envisaged operational range of ITER and DEMO-relevant plasma regimes at JT-60SA have been selected for the analysis performed in this study. Their basic features are displayed in table 1, a very detailed description is provided in [2] while [15] yields a comprehensive overview.

Scenario	#1	#2	#3	#4	#5	#6
Name	Inductive	Inductive	High density	ITER-like	High ß full-CD	High ß 300 s
Configuration	DN	SN	SN	SN	SN	SN
I_P (MA)	5.5	5.5	5.5	3.5-4.6	2.1-2.3	2.0
q_{95}	3.2	3.0	3.0	3.2-4.4	5.8-6.0	4.0
P_{add} (MW)	41	41	30	34-37	30-37	13.2
f_{Gw}	0.5	0.5	0.8	0.8	0.85-1.0	0.39
$ß_N$	3.1	3.1	2.6	2.8-3.0	4.3	3.0

Table 1: Main parameters of the six JT-60SA reference scenarios taken. DN, SN: double null, single null configurations. I_p: plasma current; q_{95}: safety factor at 95% of the poloidal magnetic flux; P_{add}: additional heating power; ratio line-averaged electron density/n_{Gw}; β_N: normalised plasma beta.

II. Strategy:

The aim of this study was to perform first a feasibility study and then to develop a system design which can be manufactured with minimized risks but covering all requirements stated in the research plan. It turned out this can be best achieved by a conceptual design composed from one baseline device covering all the essential operational needs but yielding also the option for potential extensions, upgrades and auxiliary supplements.
Following the recommendation in the research plan and also the decisions of ITER [16] and EU-DEMO [17], the initial choice for the basic design was to select "classical" pellet technology. There is a twofold reason for this decision. First, a detailed review of available alternative technologies worth serious considerations showed major shortfalls in any case, only the classical approach as applied in many fusion devices provides a sufficient and sound base. Apparently, the technology gap between different techniques has widened in recent years. While ITER's decision significantly boosted efforts for the classical technology, support of alternative approaches has been depleted. And second, evidently by using the same technology as ITER, the JT-60SA will be most suited to identify potential problems and develop relevant solutions.
A sketch of such a classical system is displayed in figure 1, showing the setup of the JET high frequency pellet injection (HFPI) system in a recent configuration, capable to launch from two different poloidal positions into the plasma. This system, described in detail in [18], serves for the JET tokamak and has tasks and capabilities close to our desired ones. As highlighted in figure 1, classical pellet systems are composed from three main components:

(1) Pellet source delivering solid fuel with the right size to the accelerating unit, pellets formed from gas in the reservoir. This can be done as batch process or in steady state,

(2) Accelerator receiving pellets from the source or cut pellets with the required size from an ice ribbon provided by the source and accelerate them to the pre-selected speed. Several classical accelerator options of different complexity are available offering different operational parameter ranges,
(3) Transfer system providing the pellet transport to the desired launch position at the plasma boundary. If required by guiding tubes, in case direct access is possible via free flight.

Usually, multiple diagnosing units are embedded within these main components for controlling the ice/pellet quality and to measure and provide the achieved pellet parameters to the tokamak feedback control and data acquisition systems.

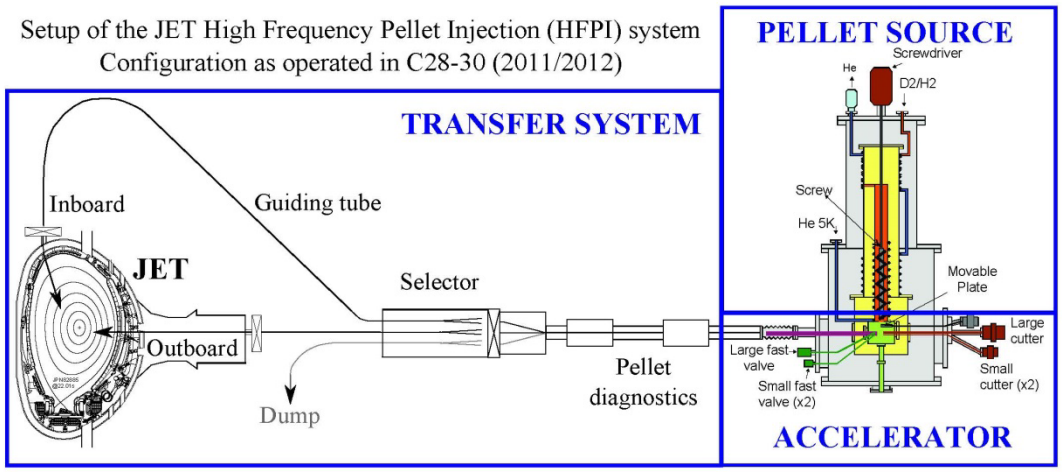

Figure 1: Setup of the JET HFPI pellet system basing on "classical" technology components like the vast majority of all systems applied in fusion research. The system is capable to deliver pellets of different size either for fuelling and ELM pacing purposes. In this initial configuration, operated during the 2011/12 campaign, pellets could be launched from both the torus in- and outboard.

To elaborate the basic layout and to serve for system optimization, mainly the expected behaviour of an analysed solution with its respect to particle fuelling was taken into account. This is due to the fact the fuelling impact of pellets is understood quite well and hence can be modelled reliable. In contrast, there are no proven quantitative models yet at hand for the ELM triggering potential of pellets. Fortunately, experimental investigation strongly indicate solutions selected for their good fuelling performance show also the most favourable behaviour with respect to their ability for triggering ELMs [19]. Modelling, at least qualitatively, agrees with this experimental finding [20]. This favours for both applications the injection from the torus inboard side rather than launch from the outboard. Inboard injection into hot plasmas, where the pellet ablation cloud is subject to a strong drift force directing into the plasma and increasing the penetration depths turned out more efficient than outboard launch (with the drift pushing pellet particles towards the plasma edge) despite the superior injection conditions (higher available speed, less mass losses) for the outboard launch [21]. Hence, we assume the best overall solution for the injection geometry with respect to all applications can be obtained by optimizing the according fuelling behaviour.
As a matter of course, a differentiation between fuelling and ELM pacing is still inevitable with respect to the pellet parameters.
These are, apart from the pellet launching location/geometry:

- Material used to produce the pellet
- Mass m_P respectively the particle content of the pellet and its shape
- Speed v_P
- Repetition rate f_P.

Notably, repetition rate and mass determine the pellet particle flux $\Gamma_P = f_P \times m_P$, the key actuation parameter for control purposes during operation.
As fuelling pellet material, pure Deuterium (D) is foreseen for the main operational phase. However, the system will be laid out to handle also pure Hydrogen (H) or any mixtures of H/D isotopologues. In addition, it is envisaged to keep also the option to use small amounts of room temperature gases like Nitrogen (N_2), Neon (Ne) or Argon (Ar) to dope the fuelling pellets. When keeping the dopant amounts sufficiently low (in the order of 1 %) it has been shown a pellet source and accelerator designed for fuelling applications can still handle doped ice and pellets [22], enabling for efficient "piggyback" supply of e.g. plasma enhancement gases [23]. Pellets dedicated to trigger ELMs will be produced most likely from the same material as the fuelling pellets in order to cause as little an unwanted fuelling side effect as possible.
For the fuelling pellet, the mass pre-set by the research plan acts already as a good indicator. For the optimisation of this parameter, according size scans have been performed in the modelling of the pellet particle deposition. The distinct pellet shape has to be adapted to or will be even settled by the chosen accelerator. For any gas gun, a cylindrical shape would fit best. In a centrifuge, the shape is essentially irrelevant. In the end, the shape is chosen to get the simplest and most reliable to fabricate. To provide optimised pacing pellets, the trigger potential has to be granted while minimizing potentially unwanted side effects like the anyway unavoidable residual fuelling. Hence, here the pellet mass has to be optimised by reducing it to an amount just sufficient to trigger an ELM while still granting a high delivery reliability. The initial pellet size has to be kept large enough, otherwise pellet losses due to acceleration and transport can compromise the high reliability inevitable for control purposes. Adversely, no modelling tools are yet at hand to predict the pellets mass threshold for ELM triggering. This threshold can, besides the mass, also depend on the pellet speed and injection location and will differ in different plasma scenarios. Consequently, the system has to provide a distinct flexibility for the available pellet masses in order to adjust this parameter in the experiment. Once again, with a pellet shape kept as simple as possible.
For the pellet speed, in all relevant cases it is expected a higher value results in deeper particle deposition and better fuelling efficiency. For the pacing application, the impact of the speed is not fully understood. On the one hand, higher speed allowing for deeper penetration was found in some cases helpful [14], on the other hand slower pellets causing a stronger local perturbation can surpass the trigger threshold more easily [20]. Thus, for ELM triggering investigations some flexibility of v_P is certainly of advantage. The speed range accessible is essentially pre-set by the accelerator chosen. Within classical technology, there is a variety of possibilities at hand [24]. One principle relies on momentum transfer from a streaming or expanding gas. In the case where the pellet dimension is smaller than the barrel diameter such a device is dubbed - blower gun. Blower guns work reliably up to very high repetition rates of 100 Hz and beyond in the speed range around 300 m/s. Higher velocities can be achieved by pneumatic gas guns where the pellet acts like a piston in the barrel driven by the expanding gas. Applying light gases like H or Helium (He) as propellant, single stage guns can achieve velocities in excess of 1000 m/s at repetition rates of several ten Hz [25]. Pellet speeds in excess of 3000 m/s can be realized by multi stage pneumatic guns, where high temperatures and pressures in the reservoir's final stage are generated by previous stage compressions. For this technique so far only quite low repetition rates have been achieved [26]. Beside gas guns, mechanical devices relying on centrifugal force acceleration have been applied. For example, the ASDEX Upgrade launcher [27] demonstrated velocities up to 1200 m/s and repetition rates beyond 80 Hz. For the envisaged operation, the

speed range up to about 1000 m/s seems to be well covered by the single stage gas gun or centrifuge option; higher speeds up to about 3000 - 4000 m/s would allow only injection at a rate capable to study single pellet effects. Evidently, the accelerator sets the range of available pellet launch speeds while the transfer system can cause restrictions to it. This becomes effectual in particular in case guiding tubes are required – and for the assumed favourable inboard injection they are inevitable. For the pellet transfer through guiding tubes, there is also some relation between pellet mass and maximum transfer speed to be taken into account as discussed later in more detail.

With respect to the repetition rates needed, a sound guidance is provided also by the research plan. For fuelling needs, $f_P = 20$ Hz is demanded in order to provide some headroom in case needed. To drive the ELM frequency up by pellets, it is requested to deliver pacing pellets up to a rate of 60 Hz.

As mentioned before, the injection location and the corresponding transfer system do play a major role for the efficiency of pellet fuelling and most likely also for ELM triggering. Roughly speaking, the potential of the physics drift effect favouring inboard launch has to be balanced against technology advantages better employable for outboard launch. In a device of the JT-60SA size and with respect to the envisaged plasma performance, it was expected the drift effect has to act in favour of the particle deposition and hence inboard launch will likely provide the best overall option. Hence, great interest has been put on the design of potential transfer systems allowing for inboard pellet injection. On the other hand, since JT-60SA is already under construction and essential parts of the torus vessel are already built and in place, stringent boundary conditions and design constraints exist. In particular, access can be granted only through a few available vessel entrance ports and space restrictions apply for the installation of the guiding tubes. From an engineering analysis and assessment, three possible injection geometry options have been identified. As displayed in figure 2, they are: outboard, top and inboard. For both outboard and inboard, at least in principle, a free flight transfer utilizing the full accelerator potential is possible. The inboard option enforces a quite intricate 3D guiding tube installation described in more detail in [28], imposing significant limitations on v_P.

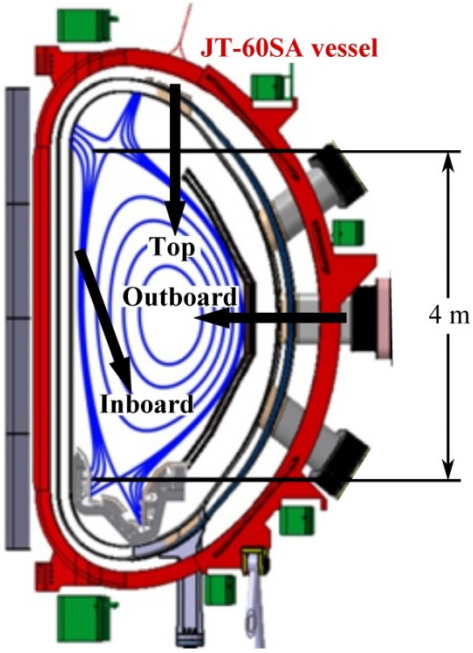

Figure 2: Poloidal cross section of JT-60SA tokamak with the three launch trajectories considered. Injection from the outboard and top can be achieved at least in principle in free flight utilizing the full accelerator potential, for inboard launch an intricate transfer system has to be employed.

III. Single pellet modelling based choice from available options:

With the available information on plasma and pellet parameter, an analysis was performed in order to find out the potential performance of the different options. This approached was based on the investigation of the expected particle deposition profile calculated for single pellets with given parameters set for every relevant scenario and for any of the considered launch position. Hence, a set of typical plasma profiles (density, temperature, magnetic configuration etc.) was taken representing the six scenarios shown in table 1. For the three injection options the according trajectories are determined by the construction-conditioned constraints; it was assumed the pellets follow straight the initial designated path. Since usually the angular scattering of the pellet trajectories is small, this effect has been neglected.
Operation in D was assumed, the same assumption was made for the pellet material. With a pellet size of Ø = l = 2.4 mm as defined in the research plan, this yields $m_P = 6.5 \times 10^{20}$ D atoms. Besides this reference case, also the option of an "oversized" pellets with $m_P = 4 \times 10^{21}$ D atoms was analysed in order to sound out how larger pellets could help to improve the fuelling efficiency.
To complete the parameter set, information about the achievable pellet speeds for the different injection configurations was needed. For the outboard launch option it is assumed free flight injection can be established and hence the maximum speed can be the full accelerator potential. Reflecting the typical performance of double stage gas guns, a range from 2000 to 4000 m/s was taken [26].
For the inboard guiding tube with multiple bends, in a first step the effective bend radius R_{eff} was estimated. In order to provide redundancy, two separate tubes will be installed; one in sector P7 and one in sector P12. Initial and final sections of both tubes are identical, just the middle section is a bit more favourable for the P12 variant. However, these differences are minor and for both inboard option $R_{eff} = 0.4$ m was taken. To determine the maximum (critical) pellet transfer speed through we used the empirical "AUG calibrated" relation [17]

$$v_c = 36.4 \left[\frac{m}{s}\right] \sqrt{\frac{R_{eff}}{l}}$$

yielding 470 m/s for $R_{eff} = 0.4$ m and l = 2.4 mm. The relation is basing on the assumption that for a pellet sliding along a contour line of radius R_{eff} the centrifugal forces are balanced by the critical yield strength σ_c. For a cubic pellet with side length l this yields

$$v_c = \sqrt{\frac{\sigma_c R}{\rho L}}$$

with ρ the pellet density. Taking for D ice at 10 - 12 K $\rho = 200 \frac{kg}{m^3}$ [24] and $\sigma_c = 0.45\ MPa$ as maximum yield strenght before pellet destruction sets in ("necking stress" fig. 6.6. in [29]), $\sqrt{\frac{\sigma_c}{\rho}} \approx 47.4 \frac{m}{s}$ is found. This is close to the value we determined for the looping type transfer system installed and operated at ASDEX Upgrade for about 20 years with $R_{eff} = 1.5$ m, where for cubic l = 2.0 mm D pellet a critical speed of 1000 m/s was found. This somewhat reduced performance is possibly is due to an extrusion process not yet fully optimized and hence resulting in a somewhat deteriorated ice quality. Possibly, this might be related to the fact material properties are measured from samples better compounded than the pellet ice and could hint for enhancement potential in the way pellets are produced for fusion applications. Nonetheless, the factual achievement was taken into account by reducing v_C calculated from the material properties by about 1.3 times.

To recheck and further substantiate this "calibrated" relation, a comparison to data from a couple of well analysed transfer systems was performed. The result is shown in figure 3. It displays the relation between the effective (or in some cases the minimum) bend radius and the critical pellet speed. Solid lines refer to the relation for four different values of l. The red dot represents the ASDEX Upgrade looping used for the calibration (cubic l = 2.0 mm pellets), of course fitting exactly to the calculated value. A wide parameter range is covered by the investigations of Combs et al. [30] providing data from different operating devices (ORNL data base, vertical black bars and grey area) and the ITER mock-up tests (vertical blue bars). As well, the critical speed observed for the JET HFPI outboard launch guide tube is indicated [31] (grey horizontal bar). The EAST HFS injection line performance for Ø = l = 2.0 mm pellets [32] (green horizontal bar) is added, too. Finally, the star represents the expected maximum pellet speed to be expected for reference size pellets launched from the inboard. To sound out if a more tight speed restriction would deteriorate the inboard fuelling performance significantly, a safer low speed option with 200 m/s was also considered. Obviously, the considered launch speed range for inboard pellet injection is well covered by available accelerator technology.
For the top launch option, free flight injection is possible in principle. However, in reality this might require efforts considered inappropriate. A dedicated technical solution was not yet worked out. Here, pellet speeds of 470 and 2000 m/s are assumed for the modelling, thought bordering well the range of reasonably possible set ups.

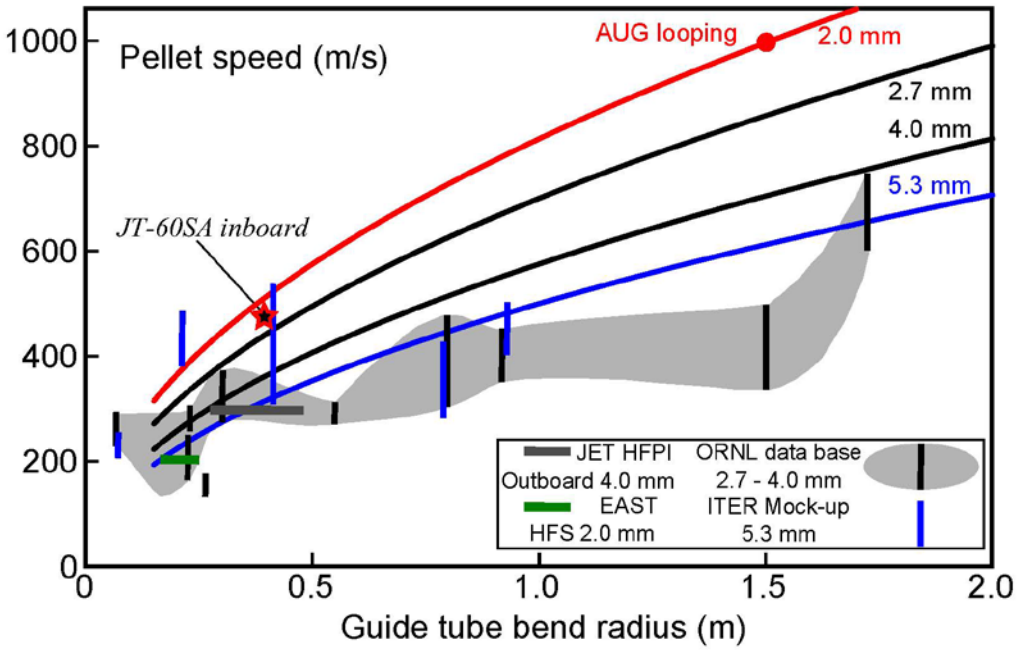

Figure 3: Maximum pellet transfer speed versus (effective) bend radius of the guide tube. Values calculated for different pellet sizes using the "AUG calibrated relation" (solid curves). Data from the ASDEX Upgrade system (red dot), the ORNL data base (black vertical bars and grey shaded area), the ITER mock-up (blue vertical bars), the JET HFPI outboard tube (grey horizontal bar) and the EAST mock-up (green horizontal bar). The red star represents the expected performance of the JT-60SA inboard launch system.

With the parameter set derived as discussed, ablation and fuelling simulations have been carried out by means of the currently most advanced tool, the HPI2 code. The code computes the pellet ablation taking into account thermal ions and electrons and the supra thermal ions generated by the plasma heating systems. It is valid for any considered magnetic and plasma configuration [33]. The employed model for the plasmoid drift altering the initial ablation profile into the final particle deposition profile is based on the compensation of the cloud polarization by parallel currents [34]. For code benchmarking, experimental data from the international pellet ablation

database [35] assembling data from several tokamaks (JET, Tore Supra, DIII-D, FTU, TFTR, ASDEX Upgrade, JIPP T-IIU, RTP and T-10) of different magnetic configurations and auxiliary heating were taken. In order to assess the potential capabilities of the pellet fuelling system, code runs have been performed covering the entire range of plausible combinations of injection geometry and pellet speed. Hence, considered cases assume high speed launch from the outboard but only moderate velocity for the inboard injection. One typical example for such a code run, analysing the injection of a single pellet into steady target plasma, is shown in figure 4. The example displays results for a reference size pellet (m_P = 6.5 x 10^{20} D) with a speed of 470 m/s from the inboard into a scenario 2 plasma. Shown in the upper left is the injection configuration with a pellet trajectory intersecting the separatrix at a radial position of R_V = 1.80 m at z = 0.63 m above mid plane and tilted by 70° with respect to the horizontal mid plane. In the simulation, a spherical pellet owing a diameter of 2.74 mm was assumed. The resulting pellet particle deposition profile with the maximum's position marked versus the normalized plasma radius is plotted in the upper right box. In the lower boxes, the impact of the particle deposition on both the electron density (left) and temperature (right) profiles is shown, displaying respective profiles before and immediately after the pellet. Notably, this modelling did not take into account the effect of ELMs potentially triggered by the pellets.

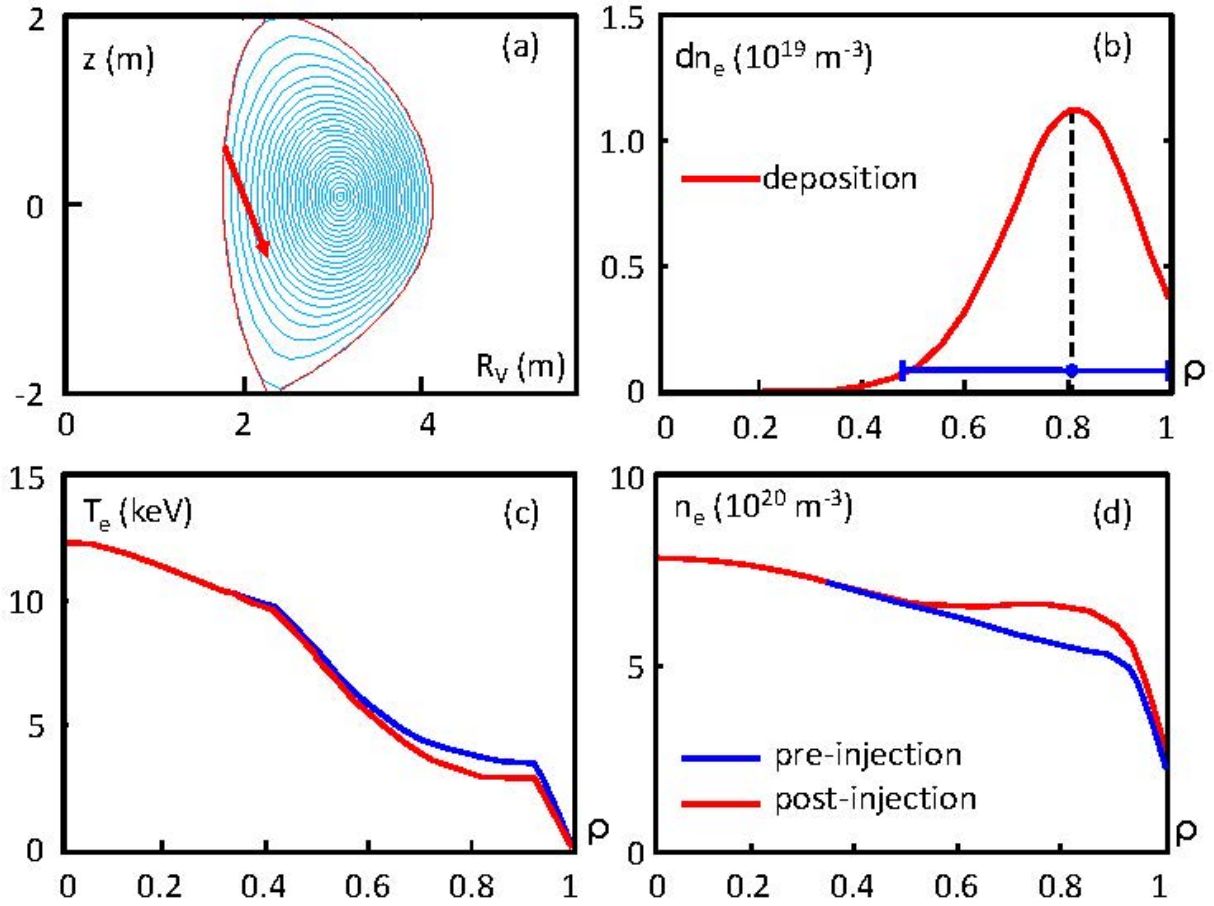

Figure 4: Pellet particle ablation and drift simulation with the HPI2 code for scenario 2 in the case of a „reference" size pellet (m_P = 6.5 x 10^{20} D) injected from the inboard with a speed of 470 m/s: (a) injection geometry; (b) pellet deposition profile versus normalized radius with peak deposition rate marked; (c) pre- and post-injection electron temperature profiles; (d) the same for the electron density.

Essential results on pellet particle deposition for all the six scenarios and pellet characteristics considered reasonable are summarized in figure 5. In its upper part it displays the deposition depths of the pellets, filled dots represent the location of the main maxima and bars the deposition profile extension until 0.1 times this value. In some of the outbaord launch cases, the drift directed towards the outward is hindered by the q = 2 surface (typically located at $\rho \approx 0.82$); the resulting congestion of the pellet particles leading to a "secondary-bump" in the deposition profile, significantly smaller than the main peak. The location of this peak is indicated by the open circles. However, the magnitude of this effect depends very strongly on the details of the simulation and was regarded as too dicey for a dependend reliable fuelling performance. The lower box in figure 5 shows the according fuelling efficiencies ε, the fraction of pellet particles deposited within the confined plasma inside the separatrix at the time the pellet is fully ablated. The missing fraction indicates for the amount of prompt losses; a significant deviation of ε from unity hints thus for a very unfavourable fuelling performance.

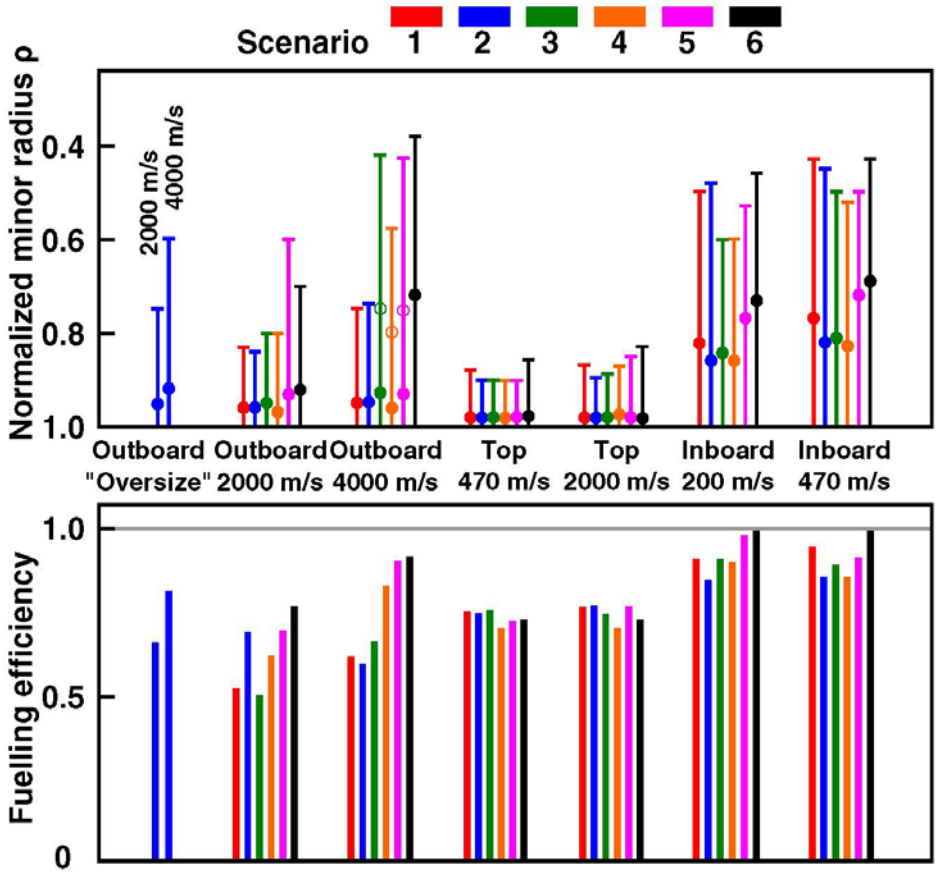

Figure 5: Upper: particle deposition depths calculated for different pellet launch sites and speeds for the considered target scenarios. All assuming D pellets with reference mass (m_P = 6.5 x 10^{20} atoms) except the case indicated "Oversize" using 4 x 10^{21} atoms. Filled dots represent the absolute maxima of the deposition profile, open dots smaller secondary peaks occurring under some conditions; bars denote the deposition profile extension until 0.1 times the maximum value. Lower: According fuelling efficiencies (ε ≡ deposited particles inside separatrix at pellet burn out / m_P).

It clearly turned out that the injection configuration is most important feature for the fuelling characteristics and inboard launch provides the best suitable solution despite its speed restriction

and the not fully optimized trajectory with respect to the flux tube geometry. Fortunately, the speed sensitivity for inboard launch is modest, hence more severe speed restrictions than assumed will not cause major performance losses. As can be seen from the ε calculated, outboard and top launch is always hampered by significant instant losses. Strikingly, the significant advantage of the inboard configuration holds for any scenario considered. It is only the outboard launch at very high speed by any chance reaching a similar performance in case the pellet can reach the q = 2 surface. This solution is regarded worthwile for physics investigations but thought unfit as baseline fuelling solution. Injection from the top is not favourable in any case. Finally, the discrepancy in fuelling efficiency between inboard cases with a rather deep perticle deposition and the situation where the pellet deposits particles close to the edge will most likely become even larger under the influence of the ELMs. It is well known ELMs causing a transient loss of the edge transport barrier mainly affect the edge and pedestal region [36]. Hence, pellet particles deposited close to the separatrix will be lost more easily than their counterparts arriving deeper inside the plasma column. Derogating shallow deposition much more than deeper profiles, ELMs will make inboard injection even more favourable as outboard or top injection.
With the results for any of the six scenarios under consideration unanimously accounting for inboard launch to provide the best fuelling perormance, thus a well settled base for qualifying the expected fuelling performance is formed. Hence, as a main conclusion from the single pellet modelling approach, it was opted to go for the inboard launch as prime choice. Here, even in case the estimated transfer speed of 470 m/s cannot fully be achieved, the best overall performance in experiments aiming on steady fuelling towards high target densities can be expected. The option for a set up enabling pellet injection at high speed in free fligth from the outboard could yield a possibility for sophisticated physics investigations on pellet and particle transport physics and also foster further technology R&D. However, it is unlikely to facilitate the full requirements postulated in the research plan. Consequently, the system design worked out in this study was focussed on the prime choice inboard.

IV. Design layout of main system components:

After a start up of pellet injection experiments with a single system, the research plan assignes the full coverage of all requirements to finally three pellet launchers. Thus, obviously for the initial system a full simultaneous supply with pellets acting for fuelling and pacing applications is not a must. Nevertheless, the presented design for the (first) system is providing the potential to act as sole pellet device for all needs. Furthermore, this design allows to start up in a simple configuration, providing an upgrade towards a flexible multi purpose system. The design proposal presented in the following aimed to account for all the existing restrictions and boundary conditions while providing a tool able to cover all the needs for JT-60SA's demanding physics and engineering tasks. Since this system has to be integrated into a device already under construction, the design started from the component facing the most stringent restrictions – the transfer system – and adopted the other components accordingly.

IV.I Transfer system

For the system the inboard launch option has to have highest priority. The in-vessel part of this track is already fixed, the design drawing is presented in figure 6. The challenging character of the solution employing many tube bends is evident, due to this it is estimated fuelling pellets can be transfered in good order only up to a speed of 470 m/s. Possibly, pellets smaller as the reference size can be used for ELM pacing; this could allow for sligthly higher velocities. On the other hand, provisions has to be taken in case reliable transfer can be achieved only at a somewhat lower pellet speed. Correspondingly, to match the technical capabilities of the transfer system adequately, the pellet speed range 200 – 600 m/s had to be covered. As a matter of course, both possible variants for tube installation have to be implemented for safety reduncancy

and/or to allow simultaneous injection from different launchers. For the start up, the P12 variant is more suited while the P7 option provides a back up solution. To the best advantage for both variants, also a nearby vessel access capable for outboard launch will be provided as well. To minimize pellet break up and mass losses, the overall travelling distance between accelerator and plasma has to be kept as short as possible. Hence, it is foreseen to place the accelerator inside the torus hall as close to the vessel as possible. An assessment of available sites for launcher installation yielded a total length L of the transfer system of about 16 m. For the start up phase and most likely also under regular operational conditions the accelerator will be connected directly to the inboard track. To grant some flexibility, an option will be provided to use a route for outboard injection, too. For the outboard pellet path, due to the anyway restrictred pellet speed, the initial part can be a guiding tube as well. Changing between both options can than simply be done by backfitting the tubes. Even more flexibility can be achieved when allowing switching between tracks within a pellet train. Designs for according selectors are available, e.g. a four way selector (three in vessel guiding tube lines and a pellet dump) has been used for the JET HFPI [31]. An even more sophisticated system is currently developed at ORNL for the ITER pellet system [37]. Such systems can manage switching between tracks within less than 1 s.

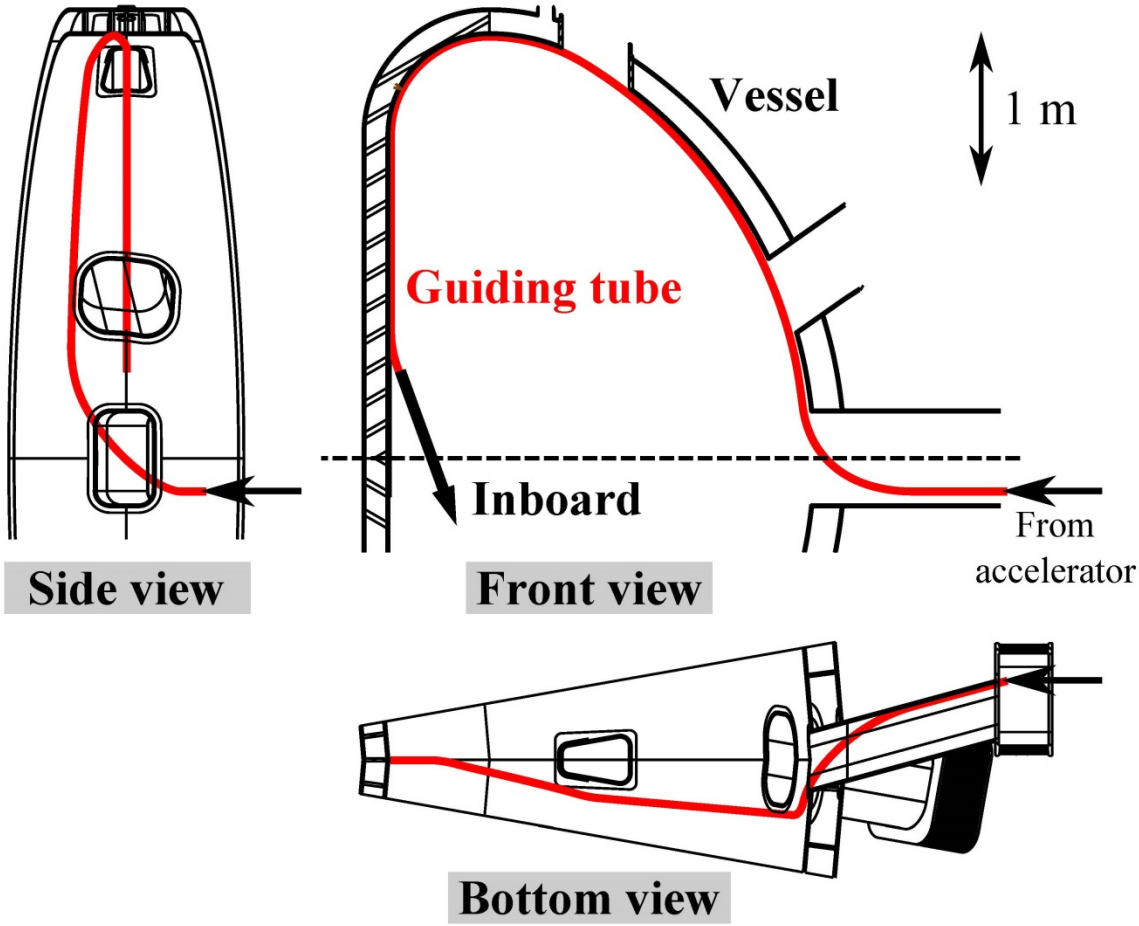

Figure 6: Guiding tube geometry installed inside the JT-60SA vessel for pellet inboard injection. Multiple bends of the guiding tube are expected to impose a limit of about 470 m/s to the maximum injection speed.

IV.II: Pellet source

Technology and design for a source required to deliver pellets steady-state or at least for sequences lasting sufficiently long (> 100 s) for the size range and with a mass throughput need for the JT-60SA system fortunately is already at hand. Once again, developments of pellet extruders undertaken for the JET HFPI and for the ITER system do well match our needs. The extruder built for the JET HFPI demonstrated reliable and persistent pellet delivery already under the harsh conditions of an operating fusion device. Its layout is suitable and demonstrated truly steady state operation despite JET can operate with pulsed plasma lasting up to several 10 s only. It can deliver selectively pellets either for fuelling or pacing purposes – bot not both simultaneously. This restriction is pursued to be avoided in our design by employing separate pacing and fuelling systems operated in parallel. For the JET HFPI system in fuelling mode, cylindrical pellets are delivered with a diameter of 4.0 mm and an adjustable lenght. Pellets can be formed either by pure hydrogen or deuterium, in the latter case m_P can be varied from 2 to 4 x 10^{20} atoms [31]. With a repetition rate of up to 15 Hz it ows a pellet flux capability of 6 x 10^{21} s^{-1}. All these parameters are very close to the JT-60SA ones, naturally since similarly sized tokamaks do need likely fuelling capacities. Set into ELM pacing configuration, cylindrical pellets with diameter 1.2 mm, adjustable length und thus mass (m_P: 0.6 – 1.2 x 10^{20} D) can be launched at up to f_P = 50 Hz. Once again, the likely needs for JT-60SA are closely matched. With this respect, the projected JT-60SA system can benefit from the R&D investments done for the JET HFPI.
For the ITER 1:5 prototype scale extruder developed at ORNL, the situation is very similar. This unit basing on a twin-screw approach as well is a steady state device, capable to handle pellet parameters also in the requires range. Furthermore, its design allow for the use of different ice species and even mixtures of different hydrogen isotopes [38].
In conclusion, devices are already at hand for a pellet source as needed for the JT-60SA pellet system. For our conceptual design, it is envisaged to use several extruders simultaneously in parallel. Every extruder is dedicated to a specific task – fuelling, pacing or eventually other needs. For the fuelling extruder, production of cylindrical Ø = 2.4 mm ice is foreseen providing the option to change the pellet length from 1.2 up to 4.8 mm (l = Ø/2 to l = 2Ø since pellets with a aspect ratio of less than two have been found stable). For l = Ø, a rate of 20 Hz is prescribed. Operation with D ice will be the standard operational scheme, but the option to use H has to be kept as well. For the pacing extruder, the design forsees a fixed Ø = l = 1.2 mm and a rate of up to 50 Hz. However, the extrusion nozzel has to be laid out for a possible easy replacement by a different diameter one. In case the potential of a single extruder is found insufficient, the concept relies on the possibility to add yet another extruder of the same type for reinforcement. Within this approach it is also possible to add an extra extruder dedicated to specific R&D tasks, as e.g. the use of ice produced from fuel doped with other species. It is understood our system design approach thus relies on an accelerator capable to receive pellets simultaneously from different sources delivering pellets at different mass and frequency.

IV.III: Accelerator

To conclude the system design, an adequate accelerator had to be chosen, able to master all the requirements and boundary conditions coming from source and transfer system. As previously stated, candidate systems have been the blower gun, centrifuge and single and double (or multiple) stage gas guns. The blower gun is disregarded, here the available speed is considered not suitable since it would restrict the operational range even further. The option to use a double (multiple) stage gas gun could be applied for outboard launching at very high speed. This is a possible set up allowing investigating pellet ablation physics and related transport effects under extraordinary conditions. However, due to the low repetition rate for this technology, it is more

adapted to a situation where every pellet performs a single experiment rather than for steady state and persisting fuelling investigations. Consequently, for the initial pellet system design, this solution was disregarded, too.
This keeps only the options single stage gas gun and centrifuge – both techniques have proven able to manage the required pellet parameters. Our decision was to go for the centrifuge solution for three main reasons. The first one is the higher precision of the pellet speed; resulting pellet trains arriving with a regular and more predictable pattern do fit better to the feed back control requirements. A comparison unveiled gas guns can show a launch speed scatter $\delta v \equiv \Delta v_P/\langle v_P \rangle$ (with $\langle v_P \rangle$ the averaged speed and $\pm\Delta v_P$ the range of launch speed variations) of about 0.1 while for a centrifuge $\Delta v_P/\langle v_P \rangle < 0.005$ can be achieved [39]. The reason for this is the strong mass dependence of the acceleration force in a gas gun [40] while there is no such dependence for the centrifuge (details in next chapter and appendix). A moderate scatter of the pellet launch speed can cause a very strong scatter in the frequency of the arriving pellets, f^A_P after tube transfer. E.g. in the case for the extreme cases a fast pellet ($v_P = \langle v_P \rangle + \Delta v_P$) is followed by a slow pellet ($v_P = \langle v_P \rangle - \Delta v_P$) or vice versa

$$1/f_P^A = 1/f_P \pm \frac{2L}{\langle v_P \rangle}\left(\frac{\delta v}{1 - \delta v^2}\right)$$

with the "+" case referring to "fast followed by slow" and "-" for "slow followed by fast". The expression becoming negative indicates pellets starts even overtaking in the tube. Assuming L = 16 m and $\langle v_P \rangle$ = 300 m/s, thus for a gas gun (δ = 0.1) for the ELM pacing (f_P = 60 Hz) f^A_P = 36 - 170 Hz and for fuelling (f_P = 20 Hz) f^A_P = 16.5 - 25.5 Hz an unacceptably high imprecision would result. In contrast for a centrifuge (δ = 0.005), respective f^A_P values of 58 - 62 and 19.8 – 20.2 Hz seem quite acceptable. Furthermore, with a centrifuge $\langle v_P \rangle$ can be matched much better to the critical transfer speed. The second reason for choosing the centrifuge is the ability of employing multiple sources for pellet delivery simultaneously, even using extruders producing differently sized pellets. For example, the former JET centrifuge could host up to six extruders simultaneously [41]. Thirdly, a centrifuge avoids the loads imposed by the propellant gas employed in a gas gun. Finally, a centrifuge can easily master all reasonable pellet shapes providing some headroom for the optimization of the extruders.
However, one principle drawback related to the centrifuge principle had to be taken into account and handled properly. Due to the revolving mechanics allowing successful pellet launch only at certain times during the cycle, pellet launch at an arbitrary time or at any frequency is not possible. Pellet launch rates must fulfil a synchronization condition with the revolving frequency f_C; $f_P = M \times f_C/N$ with N = integer and M integer ≤ number of accelerator arms. Furthermore, since the acceleration force is related to f_C, a relation between f_C and v_P exists. Hence, the details of the centrifuge layout have to be well matched to the requirements and the envisaged pellet parameter range.

V. Optimizing the centrifuge launcher:

In order to optimize the centrifuge layout for the requirements of JT-60SA, taking into account the boundary conditions caused by the transfer system and the need for simultaneous pellet delivery from different extruders, a refined design was elaborated basing on the experience from previous stop cylinder centrifuges developed for ASDEX Upgrade [27], JT-60U [42] and JET [41]. A 3D sketch of the ASDEX Upgrade system, equipped with a single batch extruder only, is shown in figure 7. Our design has been optimized in order to meet the following operational parameters. Pellet speed range 200 – 500 m/s to match the expected inboard speed capabilities. 20 Hz rate for the fuelling system since such rates have been already demonstrated; 50 Hz for the pacing extruder, a value already found hard to achieve for the JET HFPI [31]. Like the three

reference systems the JT-60SA centrifuge will run with 2 outer accelerator arms, but in contrast to them it will have 2 inner acceleration arms and hence will use both outer arms for the acceleration. This allows for a pellet rate of up to twice the revolving frequency. For the start-up configuration, two pellet sources are foreseen, one for fuelling and one for pacing purposes. In case, it also can be operated either with 2 fuelling or 2 pacing extruders in order to double the flux, respectively frequency, for the according task. Finally, it is foreseen to install up to 6 extruders on the centrifuge vessel – in a design like that one used for the JET centrifuge [43]. It is assumed the achievable precision for the feed in of the pellets from the source to the stop cylinder is 2 ms; previous systems working up to f_C = 300 Hz achieved already the accordingly required precision of 3.3 ms without dedicated efforts.

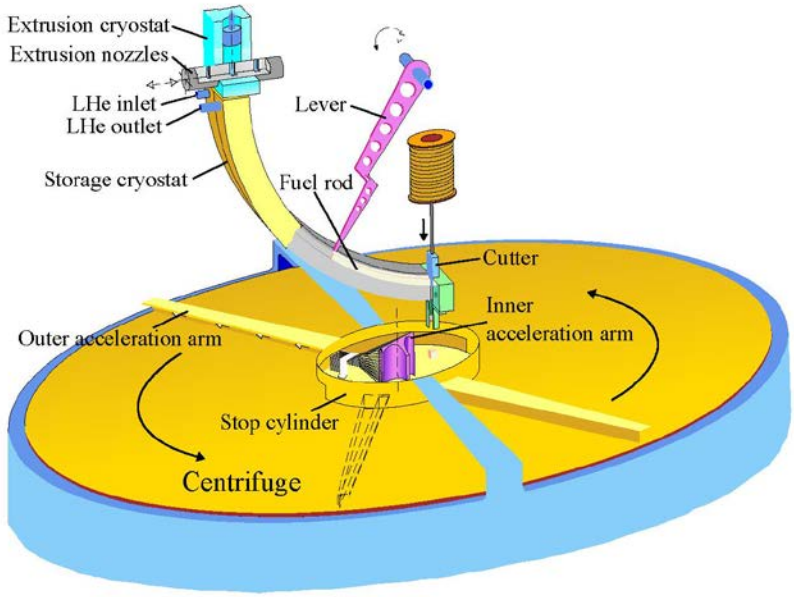

Figure 7: 3D sketch of the ASDEX Upgrade stop cylinder centrifuge launcher, equipped with a single batch extruder. Due to installation of a single inner acceleration arm, pellets can be accelerated only in one of the two available outer acceleration arms restricting the maximum pellet rate to the centrifuge revolution frequency.

A feed-in time precision t_f < 2 ms and an acceleration scheme relying on two inner arms would allow for, due to the requirements for fulfilling the relation $t_f < 1/2f_C$, a pellet frequency up to 500 Hz. Consequently, the centrifuge will be laid out for a maximum f_C = 250 Hz. For the radius r_0 of the stop cylinder, we consider a value of 0.04 m as appropriate. This value takes into account the experience from the reference systems, expected to yield the required guiding force. The length R of the outer accelerator arm can then be calculated by adjusting the maximum foreseen values of f_C and v_P (see appendix) as

$$R = \frac{1}{\sqrt{2}}\sqrt{\left(\frac{v_P}{2\pi f_C}\right)^2 + {r_0}^2} = \frac{1}{\sqrt{2}}\sqrt{\left(\frac{500\ m/s}{2\pi\ 250/s}\right)^2 + (0.04\ m)^2} = 0.2269\ m$$

For convenience, we take R = 0.23 m and get the relation v_P = 2.028 [m] x f_C. With the potential to provide a pellet rate of up to 500 Hz, this design yields sufficient headroom even in case multiple powerful extruders are employed. More likely, the pellet rate thus will be restricted by the delivery rate from the sources. Operating at the chosen high f_C allows for a precise adjustment of f_P. In fuelling experiments, for example the combination f_C = 500 Hz and f_P = 20 Hz is possible. Around 20 Hz, the synchronization condition still allows for relative small

frequency steps of a ratio 20/500 = 0.04. Consequently, also Γ_P can be thus adjusted with a final precision only. Disregarding flux changes stemming from pellet speed and mass variations, this is hence ± 2% for the fastest pellets and ± 5% for the lowest assumed pellet speed of 200 m/s. For the pellet pacing aiming at a rate of 50 Hz, the frequency can be tuned in step of about 5 Hz (50.0 Hz, 45.4 Hz, 41.7 Hz,…).

The scheme of a stop cylinder centrifuge acceleration process is shown in figure 8. In its upper part, the stop cylinder section is shown; the lower part displays the pellet trajectory while sliding on the outer arm as observed in the laboratory frame. Since the pellet path does not depend on the revolution frequency, this trajectory is identical at every f_C (the dots are plotted for equidistant times). Here, the stop cylinder principle is adapted to the use of two inner arms and the two related outer acceleration arms. The stop cylinder itself is static (but can be adjusted to tune the final pellet flight direction), inner and outer arms are fixed on the rotating centrifuge. As characteristic to the stop cylinder principle, pellets dropped into the cylinder area are picked up and driven by inner arm, sliding radially outward until they stopped by the stop cylinder. At the outlet pellets with a nil radial speed component transfer from the inner to the outer arm where final acceleration takes place. At the tip of outer arm, the pellet leaves with a well-defined exit speed and angle.

Even more details can be recognized in the upper part of figure 8. For the centrifuge hub here a radius of 0.01 m is assumed. The location of both inner acceleration arms, labelled A and B, is shown at different times displayed in blue and red (straight lines). To grant successful pellet release at right position with correct speed and direction, the pellet has to be dropped within the acceptance area. Pellets dropped outside do arrive directly at the stop cylinder outlet, causing misfiring. The two trajectories (curved solid lines) enclosing this “forbidden” area are shown; the area’s size (shaded grey in figure 8) depends on the outlet dimension.

For the chosen dimensions of stop cylinder and outer acceleration arm, the calculated acceleration angle is 139.5 ^{O}, the exit angle 45.44^{O}. The arrow displayed in the lower part of figure 8 shows the flight direction of the pellet when leaving the outer arm. Evidently, this flight direction has to point into the guiding tube entrance (or towards the plasma in case of free flight). Therefore, as in all the reference systems, a diagnostic unit for passing pellets is needed; to be mounted at the exit of the centrifuge respectively the entrance of the transfer system. During the system start up, the fine tuning of the stop cylinder adjusting the final flight direction will be committed by this detector.

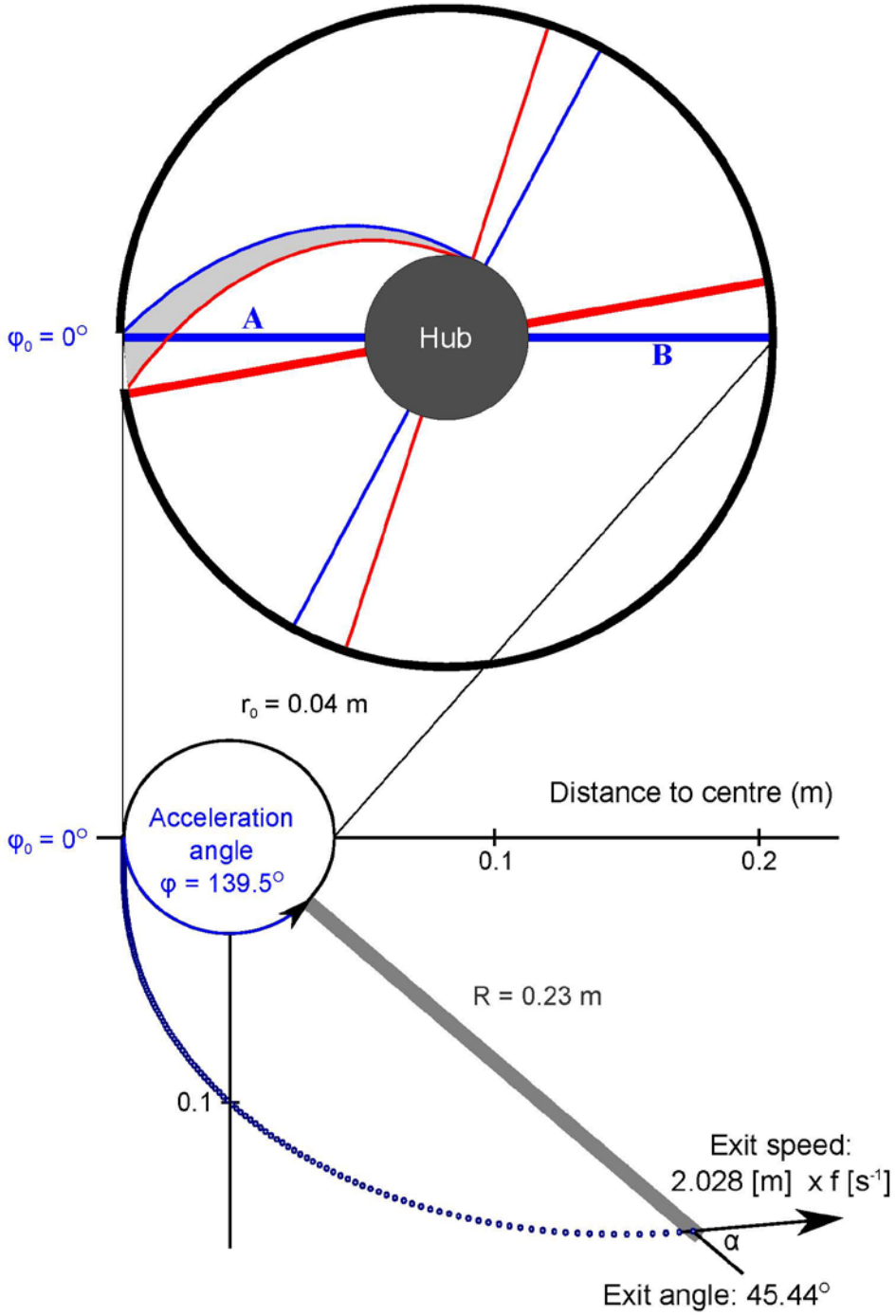

Figure 8: Upper part: Stop cylinder with the two inner acceleration arms A and B (in blue and red at different times) rotating around hub (assumed radius 0.01 m). Trajectories for pellets picked up by an inner arm enclosing the "forbidden" area (shaded grey) for feed in. Pellets inserted inside this small segment are not stopped by the stop cylinder and hence misfired. Pellets inserted elsewhere are stopped at the stop cylinder, do leave the cylinder at the outlet with nil radial speed and undergo a correct acceleration process. Lower part: Pellet path (dots represent equidistant times) on the rotating outer acceleration arm (position at pellet exit in grey) until it leaved into the direction indicated by the arrow.
Full outer acceleration angle 139.5 ^{O}, exit angle at the arms tip 45.44^{O}.

VI. Concept verification in a full modelling approach:

To conclude the conceptual design, a showcase check for the layout parameters with respect to fuelling was conducted. To do so, a full modelling approach was made. For this, the JT-60SA pellet injection geometry was implemented in the JINTRAC suite of codes and used in combination with the HPI2 module [34]. The HPI2 module calculates the pellet impact on the plasma taking into account ablation and ∇B-drift of the cloud. As initial plasma configuration scenario 2 was taken (moderate density inductive H-mode plasma, I_P = 5.5 MA and B_t = 2.25 T). Keeping the input power constant (24 MW positive NBI, 10 MW negative NBI and 7 MW ECRH), a fully predictive simulation was performed [44] using the Bohm/gyro-Bohm transport model [45]. For the code run shown in figure 9, the foreseen inboard fuelling configuration was adopted with reference size pellet launch at a speed of 470 m/s. Then, a pellet train is added, starting with a yet low f_P of 3.7 Hz. With $1/f_P$ obviously still in the range of the plasma energy and particle confinement times, the pellet impact on density, temperatures and confinement remain transient and no significant persistent changes are found. Once quasi-static conditions are achieved, the pellet rate is raised in two steps to finally 11.1 Hz. With the final rate, similar to the value estimated and stated already in the research plan as reasonable, the core density levels out at about 1.3 x n_{Gw}. Thus, this modelling confirms the pellet system parameters foreseen are can be expected to cover the fueling needs, i.e. to manage the transfer from an initial situation with moderate density to a final one with the core density in a reactor relevant range.

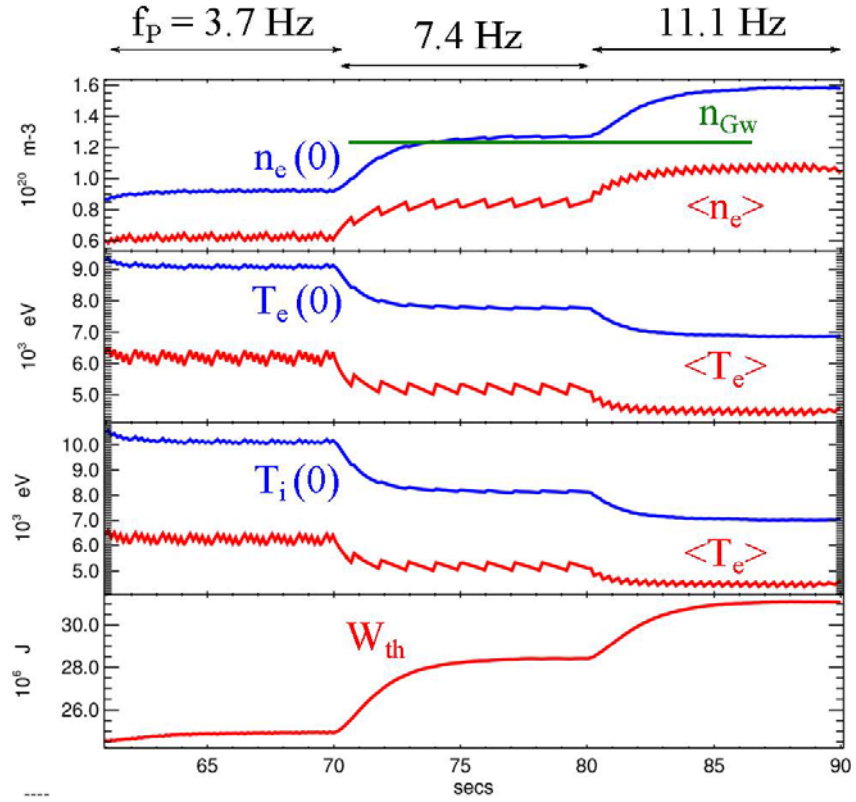

Figure 9: JETTO modelling of a fuelling sequence transferring scenario 2 to scenario 3 (inductive H-mode from moderate to high density). Assuming inboard reference size pellet injection with v_p = 470 m/s, train with increasing f_P. The increasing pellet particle flux rises the core density well beyond n_{Gw}.

VII: Summary and Outlook

System	Start-up configuration	Possible extension
Source	2 steady state extruders Operation in D, alternatively in H Fuelling: Ø = 2.4mm, l = 1.2 – 4.8 mm m_P = 3.3 – 13.0 x 10^{20} atoms (for D) f_P: up to 20 Hz (at l = 2.4 mm) Γ_P: up to 1.3 x 10^{22} /s (for D) Pacing: Ø = l = 1.2 mm m_P = 0. 8 x 10^{20} atoms (for D) f_P: up to 50 Hz	Up to 4 extruder Any combination of fuelling, pacing and test extruders Operation with HD mixtures, eventually with doped ice Γ_P: up to 5 x 10^{22} /s (for D) Exchangeable nozzel with different Ø f_P: up to 200 Hz
Accelerator	Centrifuge (stop cylinder double arm) f_C = 100 - 250 Hz v_P = 200 – 500 m/s f_P: up to 2 x f_C = 200 - 500 Hz	f_C up to design/material limits of outer arm v_P: up to 800 – 1200 m/s (as achieved reference systems) Multi stage gun (outboard launch) v_P = 2000 – 4000 m/s f_P < 1 Hz
Transfer system	Inboard (tilted by 70^o) Guiding tubes – two variants	Outboard (horizontal) Free flight Use full potential of centrifuge or multi stage gas gun

Table 2: Main parameters of the itemized JT-60SA pellet system order for the envisaged start-up configurations and for possible upgrades and extensions or alterations.

A comprehensive overview of the design elaborated for the JT-60SA pellet system, itemized with respect to the three main components, can be found in table 2. It displays the parameters foreseen for the system start-up but provides also information on possible upgrades, extensions or alterations. At present, the installation of both variants of the inboard guiding tubes is already in progress. As well, places for the launcher installation in the torus hall and access ports for possible outboard injection paths are reserved. A project plan is in preparation, aiming on a detailed component design enabling to initiate manufacturing or ordering.
Modelling efforts are under way to analyse the stability of the pellet imposed local perturbations. For example, it is well known pellet deposition modifying density, temperature and current profiles can trigger the growth of instability. Such instabilities can have a detrimental impact on the confinement and hamper fuelling efficiency. With the system layout providing sufficient headroom for adapting the pellet parameters accordingly, it is thought capable to handle measures needed to avoid such instabilities. An instructive example has been the avoidance of NTM instabilities in JET, achieved by an according tailoring of pellet flux and plasma heating

[46]. With this respect, those stability analyses can aid the efficient planning of the initial fuelling experiments once the pellet system has become operational.

Acknowledgment

This work has been carried out within the framework of the EUROfusion Consortium and has received funding from the Euratom research and training programme 2014 – 2018 under grant agreement No 633053. The views and opinions expressed herein do not necessarily reflect those of the European Commission.

Appendix

The acceleration of a pellet on a rotating straight arm can be considered as the motion of a "pearl on a rotating stick" discussed in textbooks on Lagrangian dynamics [47]. Considered is the acceleration of a pellet with mass m_P on a straight arm, rotating with a constant angular velocity ω. Assuming the motion is within a plane, an appropriate choice are the coordinates r for the radial distance and the angle φ. This gives the relations with respect to Cartesian coordinates x and y

$$x = r \cos \varphi \text{ and } y = r \sin \varphi.$$

Since the pellet is constraint to stay on the arm, we get one equation of constraint

$$\varphi - \omega t = 0,$$

reducing the two degrees of freedom to a single one. Applying this rheonome equation of constraint yields for the generalized coordinates

$$x(t) = r \cos(\omega t) \text{ and } y(t) = r \sin(\omega t).$$

For the time derivatives we get

$$\dot{x} = \dot{r} \cos(\omega t) - r\omega \sin(\omega t) \text{ and } \dot{y} = \dot{r} \sin(\omega t) + r\omega \cos(\omega t)$$

Since there is no potential energy involved (neglecting gravity) the Lagrangian L is simply the kinetic energy and hence

$$L = \frac{1}{2} m_p(\dot{x}^2 + \dot{y}^2) = \frac{1}{2} m_p(\dot{r}^2 + r^2\omega^2)$$

Applying Lagrange's equation

$$0 = \frac{d}{dt}\frac{\partial L}{\partial \dot{r}} - \frac{\partial L}{\partial r} = \frac{d}{dt}\left(m_p \dot{r}\right) - m_p r\omega^2$$

we get the equation of motion

$$\ddot{r} = \omega^2 r$$

with the general solution

$$r(t) = Ae^{\omega t} + Be^{-\omega t}\,;\ \dot{r}(t) = A\omega e^{\omega t} - B\omega e^{-\omega t}$$

Taking the initial conditions $r(t_0) = r_0$ and $v(t_0) = 0$ yields

$$r_0 = A + B \text{ and } 0 = A - B \rightarrow A = B = \frac{r_0}{2}$$

and

$$r(t) = \frac{r_0}{2}\left(e^{\omega t} + e^{-\omega t}\right) = r_0 \cosh(\omega t)\,;\ \dot{r}(t) = \omega r_0 \sinh(\omega t)$$

Since r(t) can also be expressed as

$$r(\varphi) = \frac{r_0}{2}\,(e^{\varphi} + e^{-\varphi})$$

the pellet trajectory is not dependent on ω.
The pellet is moving with steadily increasing acceleration to the outside while its total = kinetic energy continuously grows as

$$\begin{aligned} E_{tot}(t) = E_{kin}(t) &= \frac{1}{2}\, m_p\, (\dot{r}^2 + r^2\omega^2) \\ &= \frac{1}{2}\, m_p \left\{ \frac{\omega^2\, r_0^2}{4}(e^{2\omega t} + e^{-2\omega t} - 2) + \frac{\omega^2\, r_0^2}{4}(e^{2\omega t} + e^{-2\omega t} + 2) \right\} \\ &= \frac{m_p\, \omega^2\, r_0^2}{2}\cosh(2\omega t) = \frac{m_p\, \omega^2\, r_0^2}{2}\,\{1 + 2\,\sinh^2(\omega t)\} \end{aligned}$$

The acceleration time T when the pellet arrives at the end of the rotating arm R is given by

$$R = r_0\,\cosh(\omega T) \quad and\ hence\ T = \frac{\operatorname{arccosh}(\frac{R}{r_0})}{\omega}$$

During T the arm passes the acceleration angle

$$\varphi = \frac{360^o}{2\pi}\,\operatorname{arccosh}(\frac{R}{r_0})$$

To calculate the final pellet speed v_P it is helpful to calculate the kinetic pellet energy gained in the frame of the rotating arm when arriving at R

$$E_{kin} = \int_{r_0}^{R} m_p\, \ddot{r}\; dr = \int_{r_0}^{R} m_p\, \omega^2\, r\, dr = \frac{m_p\, \omega^2}{2}\,(R^2 - r_0^2)$$

yielding for the final radial component of the pellet speed

$$v_R = \omega\, R \sqrt{1 - \left(\frac{r_0}{R}\right)^2} \approx \omega\, R \left\{1 - \left(\frac{r_0}{4\, R}\right)^2\right\} \quad for\ R \gg r_0$$

The perpendicular angular speed equals the speed of the arm tip

$$v_\omega = \omega\, R$$

and hence the pellet speed in the laboratory frame is

$$v_P = \sqrt{v_R^2 + v_\omega^2} = \omega\, R \sqrt{2 - \left(\frac{r_0}{R}\right)^2}$$

Reversing this relation, R can be obtained as

$$R = \frac{1}{\sqrt{2}}\sqrt{\left(\frac{v_P}{\omega}\right)^2 + {r_0}^2}$$

For the exit angle of the pellet direction after leaving the arm with respect to the arm it yields

$$\cot\alpha = \frac{v_R}{v_\omega} = \sqrt{1 - \left(\frac{r_0}{R}\right)^2}$$

References

[1] H. Shirai et al., Nucl. Fusion 57, 102002 (2017).
[2] JT-60SA Research Unit, JT-60SA Research Plan 2016
www.jt60sa.org/pdfs/JT-60SA_Res_Plan.pdf, v3.3
[3] M. Greenwald et al., Nucl. Fusion 28, 2199 (1988).
[4] P.T. Lang et al., Nucl. Fusion 52, 023017 (2012).
[5] M. Bernert et al., Plasma Phys. Control. Fusion 57, 014038 (2015).
[6] M. Keilhacker, Plasma Phys. Control. Fusion 26, 49 (1984).
[7] H. Zohm, Plasma Phys. Control. Fusion 38, 105 (1996).
[8] K. Kamiyaet al., Plasma Phys. Control. Fusion 49, S43 (2007).
[9] R.J. Hawryluk et al., Nucl. Fusion, 49, 065012, (2009).
[10] A. Loarte et al., Nucl. Fusion 54, 033007 (2014).
[11] P.T. Lang et al., Nucl. Fusion 53, 043004 (2013).
[12] P.T. Lang et al., Nuc. Fusion, 44, 665 (2004).
[13] L.R. Baylor, et al. , Phys. Rev. Lett. 110, 245001 (2013)
[14] P.T. Lang et al., Nucl. Fusion 53, 073010 (2013).
[15] G. Giruzzi et al., Nucl. Fusion 57, 085001 (2017).
[16] L.R. Baylor et al., Nucl. Fusion 47, 443 (2007).
[17] P.T. Lang et al., Fusion Engineering and Design 96/97, 123 (2015).
[18] A. Geraud et al., Fusion Eng. Des. 82, 2183 (2007).
[19] D. Frigione et al., Journal of Nuclear Materials 463, 714 (2015).
[20] S. Fututani et al., Nucl. Fusion 54, 073008 (2014).
[21] P.T. Lang et al., Phys. Rev. Lett. 79, 1487 (1997).
[22] B. Ploeckl et al., Fusion Engineering and Design 96/97, 155 (2015).
[23] P.T. Lang et al., 42rd EPS Conf., P2.127 (2015)
[24] S. Combs, Rev. Sci. Instrum. 64 (1993) 1679
[25] S. K. Combs, S. L. Milora, C. R. Foust, C. A. Foster, and D. D, Schuresko, Rev. Sci. Instrum. 56, 1173 (1985).
[26] F. Bombarda et al., State of the art and perspective of high-speed pellet injection technology, 29th SOFT2016, P4.158
[27] C. Andelfinger et al., Rev. Sci. Instr. 64, 983 (1993)
[28] P. T. Lang et al., Conceptual design of the JT-60SA pellet launching system, 29th SOFT2016, P2.19
[29] P.C. Sours, Hydrogen properties for fusion energy, University of California Press, Berkeley and Los Angeles (1986)
[30] S.K. Combs et al., Fusion Engineering and Design 75–79, 691 (2005)
[31] P.T. Lang et al., Nucl. Fusion 51, 033010 (2011)
[32] C.Z. Li et al., Fusion Engineering and Design 89, 99 (2014)
[33] B. Pégourié et al., Plasma Phys. Control. Fusion 47, 17 (2005)
[34] B. Pégourié et al., Nucl. Fusion 47, 44 (2007)
[35] L. R. Baylor et al., Nucl. Fusion 37, 445 (1997)
[36] P. A. Schneider et al., Plasma Phys. Control. Fusion 77, 014029 (2015)
[37] L.R. Baylor, Private Communication
[38] L. Degitz, „Pellet injection advances to next stage in the US“, ITER NEWSLINE 282 (September 24., 2013)
[39] B. Ploeckl et al., Fusion Engineering and Design 86, 1022 (2011)
[40] L. D. Landau and E. M. Lifshitz, Fluid Mechanics (Addison-Wesley, Reading, MA, 1959).
[41] D.J. Wilson et al., 20th IEEE/NPSS SOFE, San Diego, 86 (2003)
[42] K. Kizu et al., Fusion Engineering and Design 58–59, 331 (2001) 331
[43] P.T. Lang et al., Rev. Sci. Instr. 71, 3744 (2000)

[44] L. Garzotti et al., “Analysis of JT-60SA operational scenarios”, submitted to Nuclear Fusion.
[45] M. Erba et al., Plasma Phys. Control. Fusion 39, 261 (1997)
[46] P.T. Lang et al., Nucl. Fusion 42, 388 (2002).
[47] D. A. Wells, Theory and problems of Lagrangians dynamics, Schaum Publishing Co, New York (1967)